

Over-The-Air Clustered Wireless Federated Learning

Ayush Madhan-Sohini^{*,†}, Divin Dominic^{*,†}, Nazreen Shah[†], Ranjitha Prasad[†]

Abstract

Privacy, security and bandwidth constraints have led to the use of federated learning (FL) in wireless systems, where training a machine learning (ML) model is accomplished collaboratively, without sharing raw data. Often, such collaborative FL strategies necessitates model aggregation at a server. On the other hand, decentralised FL necessitates that participating clients reach a consensus ML model by exchanging parameter updates. In this work, we propose the over-the-air clustered wireless FL (CWFL) strategy which eliminates the need for a strong central server and yet achieves an accuracy similar to the server-based strategy, while using fewer channel uses as compared to decentralized FL. We theoretically show that at high SNRs, the convergence rate of CWFL per cluster is $\mathcal{O}(1/T)$. Using the MNIST and CIFAR datasets, we demonstrate the accuracy performance of CWFL for different number of clusters across communication rounds.

I. INTRODUCTION

Due to bandwidth-constraints and an increased demand for privacy-preserving communications, distributed wireless systems are moving away from cloud computing towards edge computing. Federated learning (FL) enables learning at the edge devices over bandwidth-constrained wireless channels, where data is processed locally at the *clients* but the model is learnt collaboratively at the server [1], [2]. The distributed framework of FL using the FedAvg algorithm was proposed in [1] with a focus on communication latency and bandwidth. In the context of wireless networks, the base station plays the role of the central server [3]. Over-the-air (OTA) parameter update transmission allows a large number of mobile devices to concurrently upload their local models by exploiting the superposition property of wireless multi-access channels (MAC). In

[†] Indraprastha Institute of Information Technology Delhi, New Delhi

* Equal Contribution.

scenarios such as D2D communications, a base station-centric architecture is unavailable due to connectivity and computational constraints and hence, decentralised wireless FL is employed in [4]. However, a fully decentralised strategy requires large number of channel uses for consensus.

Contributions: In this work, we propose a novel strategy for FL in server-free setting. We introduce OTA clustered wireless federated learning (CWFL), where clustering of clients is performed in a data-agnostic SNR-aware manner. CWFL is a hierarchical technique where clients exchange parameter updates with *cluster-heads*, and the cluster-heads in turn exchange updates among each other to achieve *consensus*. We analyse the convergence behavior of CWFL and show that CWFL demonstrates a per-cluster convergence rate of $\mathcal{O}(1/T)$, where T is the total number of communication rounds. Using the CIFAR and MNIST dataset, we demonstrate an improved robustness (fewer instances of drop in accuracy across rounds) of the CWFL framework as compared to the COTAF algorithm [5].

II. RELATED WORKS AND NOVELTY

The idea of FL was proposed as a simple aggregation based distributed learning algorithm known as FedAvg [1]. In order to tackle the issues arising from heterogeneous and non-identically distributed data (non-IID) at the clients, methods such as FedProx [6], optimal rate and adaptivity based FedPD [7], etc have been proposed. Subsequently there is an exponential growth in the literature related to FL due to its relevance in current-day technologies. Theoretical convergence guarantees of FedAvg was derived in [8]. In several practical scenarios, a powerful server may be absent, and such frameworks demand the use of decentralized FL [9]. BrainTorrent for medical applications [10], Online-Push Sum (OPS) [11], peer-to-peer cryptographic block-chain based Biscotti [12] are popular examples. In wireless communications, bandwidth is a critical bottleneck for global aggregation of the locally computed parameter updates. In general, aggregation of parameter updates entails transmitting updates from multiple clients over orthogonal time/frequency resources as proposed in [13], [14]. In contrast, over-the-air FL (OTA-FL) strategy allows clients to simultaneously transmit updates over uplink channel in a non-orthogonal manner, hence optimizing on temporal and spectral resources. OTA-FL employs analog signalling for transmission of model updates without converting updates into discrete coded symbols, while exploiting the aggregation of signals that occurs due to the nature of the shared MAC channel [5]. Model based inference in OTA MACs with theoretical guarantees is well-established [15], [16], in the absence of machine learning paradigms. Several variations of the OTA-FL algorithm

have been proposed [17], [18]. The existing method closely related to our work is [5] where the authors propose the COTAF algorithm which uses pre-coding in order to facilitate high throughput OTA FL over wireless channels.

III. SYSTEM MODEL

We consider global objective $F(\boldsymbol{\theta})$ which is a collaborative function over multiple clients with common model parameters $\boldsymbol{\theta} \in \mathbb{R}^{d \times 1}$. The distributed objective of FL is given by

$$\min_{\boldsymbol{\theta}} F(\boldsymbol{\theta}) \triangleq \sum_{k=1}^K p_k f_k(\boldsymbol{\theta}), \quad (1)$$

where $f_k(\boldsymbol{\theta}) \triangleq N_k^{-1} \sum_{i=1}^{N_k} l(\boldsymbol{\theta}; x_i)$. The local objectives $f_k(\boldsymbol{\theta})$ ($k \in \mathcal{K} \triangleq [K]$) measure the empirical risk over possibly differing data distributions at K clients. Each client has access to a local dataset \mathcal{D}_k consisting of N_k data samples, i.e., the total size of the training data is $N = \sum_{k=1}^K N_k$. Further, $p_k \geq 0$ is the weight assigned to the k -th client such that $\sum_{k=1}^K p_k = 1$. Further, $f_k(\boldsymbol{\theta})$ consists of a user specified loss function $l(\boldsymbol{\theta}; \cdot)$ where $x_i \sim \mathcal{D}_k$.

FedAvg is one of the most widely adopted FL algorithm [1], where the ML model is learnt at the server by aggregating the client parameters obtained from local data \mathcal{D}_k . In FedAvg, at time instant t , clients update the local model parameters $\boldsymbol{\theta}_k^t \in \mathbb{R}^{d \times 1}$ over E epochs and R communication rounds. The server aggregates these model parameters that are communicated to the server over a wireless channel to obtain the global parameter update at synchronization steps given in $\mathcal{H} = \{nE | n = 1, 2, \dots\}$. Local upation or aggregation occurs as follows:

$$\begin{cases} \boldsymbol{\theta}_k^{t+1} = \boldsymbol{\theta}_k^t - \eta \nabla f_k(\boldsymbol{\theta}_k^t), & \text{if } t+1 \notin \mathcal{H} \\ \boldsymbol{\theta}^{t+1} = \sum_{k=1}^K p_k \boldsymbol{\theta}_k^t, & \text{if } t+1 \in \mathcal{H} \end{cases} \quad (2)$$

where η is the learning rate and $\nabla f_k(\boldsymbol{\theta}_k^t)$ is the gradient w.r.t a mini-batch $\omega_k \in \mathcal{D}_k$. Global synchronization concludes with the update $\boldsymbol{\theta}^{t+1}$ being shared with the K clients. Decentralized setting [4] is adopted in the absence of a computationally powerful server where, the connectivity of the K devices is governed by an underlying undirected graph, $\mathcal{G}(V, L)$, where L represents the set of edges such that $L \subset \{(i, j) \in V \times V | i \neq j\}$. The set of neighbors of node $i \in V$ is denoted as $\mathcal{A}_i = \{j \in V | (i, j) \in L\}$ [4], [19], [20]. A symmetric doubly stochastic matrix $\tilde{\mathbf{W}} \in \mathbb{R}^{K \times K}$ where $\tilde{\mathbf{W}}(i, j) = \tilde{\mathbf{W}}(j, i)$ for $1 \leq i, j \leq K$ encodes the extent to which node j can affect node i , while $\tilde{\mathbf{W}}(i, j) = 0$ implies that node i and j are disconnected. In the decentralised framework, each client optimizes (1) with parameter updates from the neighboring clients only.

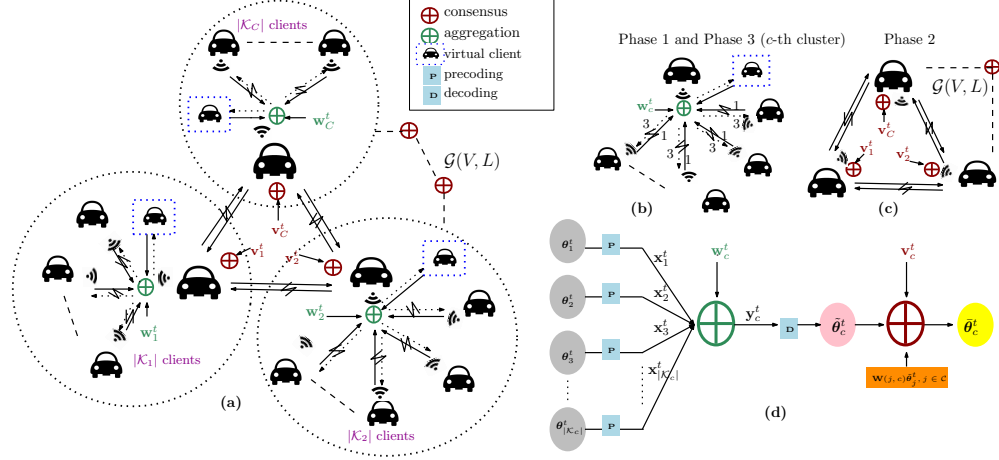


Fig. 1: Clustered wireless FL strategy is depicted in (a), individual phases in (b) and (c) and signal flow diagram in (d).

We consider the decentralised framework in [21], where each client updates its parameters at $t + 1 \in \mathcal{H}$ as

$$\theta_k^{t+1} \leftarrow \theta_k^{t+\frac{1}{2}} - \eta \nabla f_k(\theta_k^t), \quad \theta_k^{t+\frac{1}{2}} = \sum_{j=1}^K \tilde{\mathbf{W}}(k, j) \theta_j^t. \quad (3)$$

From the above, it is evident that decentralised framework requires $K(K-1)$ orthogonal channel uses in each communication round. We consider the problem of FL across K wireless devices, where the parameter updates from the clients to the server and global synchronization from server to client happens over the resource constrained uplink channel and over the downlink channel, respectively. Downlink transmission is assumed to be error-free [5]. We employ the uplink channel model where the channel output received by the server in the presence of fading at $t \in \mathcal{H}$ is given by

$$\mathbf{y}^t = \sum_{k=1}^K h_{k,s} \mathbf{x}_k^t + \mathbf{w}^t, \quad \text{where } 0 < \mathbb{E}[\|\mathbf{x}_k^t\|^2] \leq P_k, \quad (4)$$

for all k and $\mathbf{w}^t \sim \mathcal{N}(0, \sigma^2 \mathbf{I}_D)$, where σ^2 is the noise variance of the additive white Gaussian noise. The wireless link between the server, represented as s , and client k is modeled as a Rayleigh faded channel, $h_{k,s} = \sqrt{P_k} (d_0^{-1} d_{k,s})^{\zeta/2} \tilde{h}_{k,s}$, where d_0 is the reference distance, $d_{k,s}$ is the distance between devices k and s , and ζ is the path-loss co-efficient [22]. We model the channel to be stationary, i.e., the channel remains the same throughout training for all t . We

Algorithm 1: Clustered Wireless FL

Input: Dataset \mathcal{D}_k at the k -th client, \mathbf{u}_c for $c \in [C]$;

Initialize parameters at all clients;

for $t \in [T]$ **do**

if $t \in \mathcal{H}$ **then**

$\tilde{\boldsymbol{\theta}}_c^t = \sqrt{P}^{-1} \mathbf{y}_c^t$ (as given in (8)), $c \in [C]$;

 Obtain $\bar{\boldsymbol{\theta}}_c^t$ (given in (9));

 Cluster-head broadcasts $\bar{\boldsymbol{\theta}}_c^t$, i.e., $\boldsymbol{\theta}_k^{t+1} = \bar{\boldsymbol{\theta}}_c^t$;

end

if $t \notin \mathcal{H}$ **then**

 Update in parallel: $\boldsymbol{\theta}_k^{t+1} \leftarrow \boldsymbol{\theta}_k^t - \eta \nabla f_k(\boldsymbol{\theta})$;

end

end

Output: Consensus parameter: $\boldsymbol{\theta}^T = \frac{1}{C} \sum_{c=1}^C \bar{\boldsymbol{\theta}}_c^T$.

assume that the channel input is power constrained, and P_k represents the available transmission power at the k -th client. Accordingly \mathbf{x}_k^t is transmitted over the wireless channel, such that

$$\mathbf{x}_k^t = \sqrt{P_k^t} \boldsymbol{\theta}_k^t, \text{ where } P_k^t \triangleq \min(P_k, \mathbb{E}[\|\boldsymbol{\theta}_k^t\|^2]^{-1} P_k), \quad (5)$$

where $\sum_{k=1}^K P_k = P$, which leads to the overall SNR is given by $\xi = \frac{P}{\sigma^2}$. Power is allocated to each wireless device, P_k , is obtained using the water-filling solution [22], considering the effective channel strength per client-server link as $|h_{k,s}|$. Here, P_k^t is a client specific pre-coding factor that scales the model parameters as t progresses such that power constraint stated in (4) is satisfied in an expected sense. The OTA model in (4) signifies that communication is not restricted to orthogonal channels and the server has access to the shared MAC channel output. We represent the parameter updates collectively as

$$\boldsymbol{\Theta}_{[K]}^t = \left[h_{1,c}^{-1} \sqrt{P_1^t} \boldsymbol{\theta}_1^t, \dots, h_{K,c}^{-1} \sqrt{P_K^t} \boldsymbol{\theta}_K^t \right]. \quad (6)$$

IV. CLUSTERING IN WIRELESS FL

We propose clustered wireless FL (CWFL) in a server free framework, where the fundamental idea is to cluster the clients to *distribute* the tasks of a server to a *subset* of clients (cluster-heads) that are *reliably* connected to other clients in the cluster. We initiate the process of clustering by choosing the cluster-heads $\mathcal{C} \subset \mathcal{K}$ ($|\mathcal{C}| = C$). We propose per-client K-means strategy where each client executes the K-means algorithm offline, with the knowledge of topology $\mathcal{G}(V, L)$ and intra-client channels, $h_{k,j}^t$ for $k, j \in [K], k \neq j$. The per-client clustering strategy which is based on the channel SNR ξ_k leads to C centroids. The client closest to a given centroid is designated as the cluster-head. Each client is assigned to a cluster based on the distance metric, which leads to clusters with high-SNR links. These clusters have high confidence in their parameter updates. The global consensus update imposes higher weightage on the high-SNR cluster parameters, leading to reduced adverse impact of poorer channels.

Implicitly, CWFL leads to a hierarchical approach, where, in the first phase of a given round clients in each cluster communicate with their *cluster-heads* in parallel, and in the second phase the cluster-heads communicate among each other to achieve consensus as depicted in Fig. 1. In the consensus phase (phase 2), C cluster-heads communicate with each other, which implies that we need to rely on the decentralised strategy (given in (3)). Decentralised strategy involves obtaining $\boldsymbol{\theta}_c^{t+\frac{1}{2}}$ first, which is later updated using local data to obtain $\boldsymbol{\theta}_c^{t+1}$. In contrast, consensus in CWFL is preceded by an aggregation step, and it is possible to utilize local data at the cluster head (via $\nabla f_k(\boldsymbol{\theta}_k^t)$) during aggregation (Phase 1) itself. We mathematically enable this by designating a *virtual client* per cluster head such that the virtual client is connected to the cluster head via a noiseless error free channel. Further, virtual client takes the onus of local training using the data available at the cluster head \mathcal{D}_c , which makes the cluster head data free and aggregation and consensus are its only tasks for $t \in \mathcal{H}$. Accordingly, in the phase 1, the channel output at the c -th cluster-head, $\mathbf{y}_c^t \in \mathbb{R}^d$ for $t \in \mathcal{H}$ is given by

$$\mathbf{y}_c^t = \mathbf{s}_c^t + \mathbf{w}_c^t, \text{ where } \mathbf{s}_c^t = \boldsymbol{\Theta}_{[K]}^t \mathbf{H}_c \mathbf{u}_c + \boldsymbol{\Theta}_{v,[C]}^t \mathbf{1}_c, \quad (7)$$

where $\boldsymbol{\Theta}_{v,[C]}^t = [\boldsymbol{\theta}_{v,1}^t, \dots, \boldsymbol{\theta}_{v,C}^t]$ consists of parameter updates from C virtual clients, $\mathbf{1}_c$ is a binary vector such that $\mathbf{1}_c(c) = 1$ and 0 elsewhere, and diagonal matrix $\mathbf{H}_c = \text{diag}(h_{1,c}, \dots, h_{K,c})$. The OTA aggregation at the c -th cluster head, $\mathbf{s}_c^t = \sum_{k \in \mathcal{K}_c} \mathbf{x}_k^t + \boldsymbol{\theta}_{v,c}^t$, is alternately expressed using a binary cluster membership vector $\mathbf{u}_c \in \{0, 1\}^K$ for the c -th cluster. Here, $\mathbf{u}_c(k) = 1$ if the k -th client belongs to the c -th cluster and 0 otherwise. Hence, $\mathcal{K}_c \subset \mathcal{K}$ is a set that consists of

the clients in the c -th cluster such that $|\mathcal{K}_c| = \sum_{k \in \mathcal{K}_c} \mathbf{u}_c(k)$, and \mathcal{V} is the set of virtual clients. Further, $\mathbf{w}_c^t \sim \mathcal{N}(0, \sigma_c^2 \mathbf{I}_D)$ is the additive noise at the cluster head c . Given SNR ξ_c as average SNR at cluster-head c , the OTA update at $t \in \mathcal{H}$ is given as

$$\tilde{\boldsymbol{\theta}}_c^t = \sqrt{P}^{-1} \mathbf{y}_c^t = \sum_{k \in \mathcal{K}_c} p_k \boldsymbol{\theta}_k^t + \tilde{\mathbf{w}}_c^t, \quad (8)$$

where $p_k = \sqrt{P^{-1} P_k}$ if $k \in \mathcal{K}_c$ and 1 if $k \in \mathcal{V}$. In particular, we represent $\mathcal{K}_c^V = \mathcal{K}_c \cup v_c$ where v_c is the virtual client for the c -th cluster and $\tilde{\mathbf{w}}_c^t \sim \mathcal{N}(0, P^{-1} \sigma_c^2 \mathbf{I}_D)$. Each cluster-head transmits $\tilde{\boldsymbol{\theta}}_c^t$ to other cluster heads $j \in \mathcal{C}$ using the communication scheme similar to previous communication between client and cluster-head. Effectively, this leads to the consensus update (Phase 2) at the c -th cluster-head given by

$$\bar{\boldsymbol{\theta}}_c^t = \sum_{j=1}^C \mathbf{W}(j, c) \tilde{\boldsymbol{\theta}}_j^t + \tilde{\boldsymbol{\theta}}_c^t + \mathbf{v}_c^t, \quad (9)$$

where $\mathbf{v}_c^t \sim \mathcal{N}(0, \kappa_c^2 \mathbf{I}_D)$, $\mathbf{W}(j, c) = (\sum_{j, j \neq c} \xi_j)^{-1} \xi_j$ and $\mathbf{W}(c, c) = 0$ for all c , i.e., higher importance is given to clusters with larger average SNR. Note that this phase requires $C(C-1)$ channel uses which is fewer as compared to the fully decentralised scheme. In the third phase, the cluster heads concurrently transmit their updates to the clients in their respective clusters. The update process is summarized in Fig. 1 ((b) and (c)) and in Algorithm 1.

Convergence of CWFL: In this section, we demonstrate the convergence of the CWFL framework using standard assumptions of L -Lipschitz smoothness and μ -strong convexity of $f_k(\cdot)$, G -boundedness and α -bounded variance of stochastic gradients [5].

Theorem 1. *Under assumptions 1-4 given above, given constants L, μ, α_k, G, p_k , choosing $\gamma = \max(E, \frac{12L}{\mu})$ and choosing the learning rate $\eta^t = \frac{2}{\mu(\gamma+t)}$, each cluster in CWFL satisfies*

$$\mathbb{E} \|\tilde{\boldsymbol{\theta}}_c^T - \boldsymbol{\theta}^*\|^2 \leq \frac{2 \max \left(4(Q_1), \mu^2 \gamma \|\tilde{\boldsymbol{\theta}}_c^0 - \boldsymbol{\theta}^*\|^2 \right)}{\mu^2 (T + \gamma - 1)} + Q_2, \quad (10)$$

where $Q_1 = 8E^2 G^2 \sum_{k \in \mathcal{K}_c^V} p_k + 6L\Gamma + \sum_{k \in \mathcal{K}_c^V} p_k^2 \alpha_k^2$,
 $Q_2 = d(P^{-1} \sigma_c^2 + \kappa_c^2) + 3P^{-1} \sum_{j=1}^C (\mathbf{W}(c, j))^2 \left[\sum_{k_j \in \mathcal{K}_j^V} (p_{k_j})^2 + d\sigma_j^2 \right]$.

Proof. In order to prove the above, we proceed to define the virtual sequence of updates as $\tilde{\boldsymbol{\theta}}_c^{t+1} = \bar{\boldsymbol{\theta}}_c^t - \eta^t \mathbf{g}^t + \tilde{\mathbf{w}}_c^t \mathbf{1}_{t \in \mathcal{H}}$. In contrast to [5], the virtual sequence consists of the consensus update $\bar{\boldsymbol{\theta}}_c^t$ instead of $\tilde{\boldsymbol{\theta}}_c^t$ (as in [5]), i.e., the aggregated parameter update is replaced by the consensus update. Further, we split the terms similar to [5] to obtain the result as given above. If c is a SNR dominant cluster, $\sigma_c^2, \kappa_c^2 \rightarrow 0$. Further, the product, $\mathbf{W}(c, j)^2 \sigma_j^2 \approx 0$ at high SNR for

$c \neq j$, and which implies $Q_2 \approx 0$. Hence, convergence occurs as $\mathcal{O}(1/T)$. The details of the steps are provided in appendix. \square

V. EXPERIMENTS AND RESULTS

In this section, we demonstrate the performance of the proposed CWFL algorithm developed in Sec. IV. We consider the 10-class image classification task in the MNIST and the CIFAR datasets. MNIST dataset consists of 28×28 images, with 60000 training and 10000 test data samples. CIFAR dataset consists of $32 \times 32 \times 3$ images, with 50000 training and 10000 test data samples. The common ML model trained using the MNIST dataset is a neural network (NN) consisting of 4 layers with ReLU activation. For the CIFAR dataset, the common ML model consists of 6 layers, including 3×64 , 64×120 and 120×200 convolutional layers, with ReLU activation. In both architectures, each convolutional layer is followed by a 2×2 max-pooling layer, and finally by a log-softmax function. We incorporate a standard negative log likelihood (NLL) loss function $l(\cdot, \cdot)$ and SGD with a mini-batch size of $|B_k| = 64$, and the learning rate of $\eta = 0.001$ for MNIST, and with a mini-batch size of $|B_k| = 32$, and the learning rate of $\eta = 0.001$ for CIFAR datasets. Using pilot signals we ascertain if any inter-client Rayleigh faded channel is in an outage. Allowing only those wireless links that are not in outage leads to the graph topology $\mathcal{G}(V, E)$.

In the IID setting, data is randomly and equally distributed among $K = 50$ clients (for MNIST) and among $K = 27$ clients (for CIFAR). In the non-IID-iid setting, the dataset is sorted according to the value of the target classes (0-9), and divided into 200 disjoint sets. Each client ($K = 50$) receives 4 (MNIST) and 7 (CIFAR) ($K = 27$) of these sets. In order to obtain clusters for CWFL, we employ the K-means algorithm based on the SNR of the wireless links. The variance of the additive white Gaussian noise (AWGN) at each receiver is such that the overall SNR ξ is 40 dB. As a baseline, we consider the slightly modified COTAF algorithm where parameter updates (instead of update differences) are directly communicated using water-filling based power allocation. Further, we also implemented the FedProx scheme [6] in the context of wireless communication, where we add a proximal constraint to the existing optimization problem in (1) at each client, leading to $f_k^p(\boldsymbol{\theta}) \triangleq f_k(\boldsymbol{\theta}) + \frac{\mu_p}{2} \|\boldsymbol{\theta} - \boldsymbol{\theta}_g\|^2$, where $\boldsymbol{\theta}_g$ is the most recent global synchronization parameter update. We consider classification accuracy with respect to the test set as our performance metric.

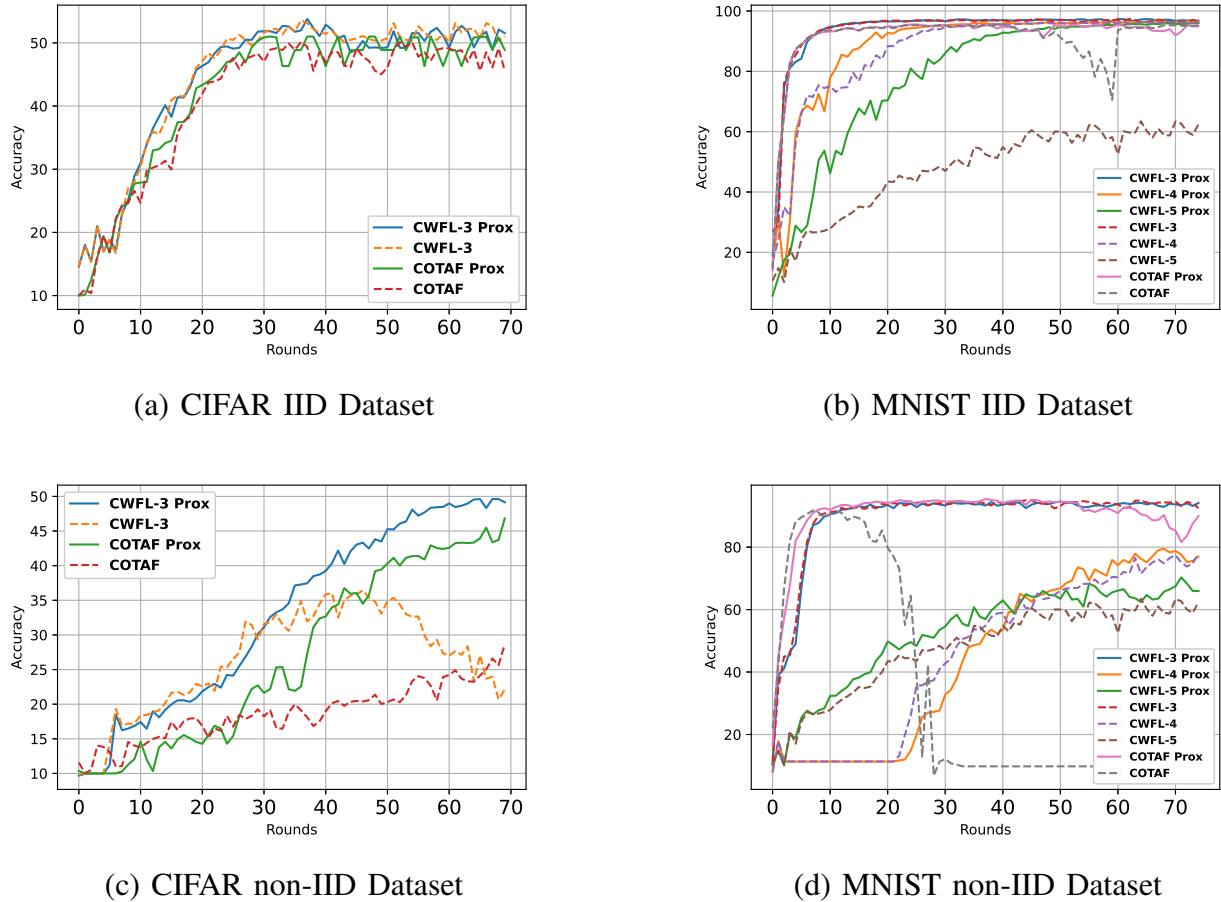


Fig. 2: Accuracy evolution as a function of communication rounds for IID and non-IID CIFAR and MNIST datasets.

In Fig. 2, we depict the evolution of accuracy across 70 – 80 communication rounds, for the IID and non-IID scenarios for both the datasets, when the clients and cluster heads are stationary, i.e., when the channel does not change across communication rounds. In the IID setting, we observe that considering 3 clusters is optimal for both datasets. In the case of CIFAR dataset, the ML model is more complex (large number of parameters to be learnt/communicated), which implies that large amounts of data is required for per-client training. Increasing the number of clusters results in overfitting since data per client is lower. Here, the proximal constraint is effective in contrast to simple ML model case (MNIST) where the constraint is marginally effective when the number of clusters is optimal. In non-IID settings, the average accuracy achieved is lower than in the IID setting, as expected and CWFL with 3-clusters is optimal. We observe that drops in

Technique	MNIST (non-IID)	CIFAR (non-IID)
COTAF	9.8	22.42
COTAF Prox	91.55	40.398
CWFL-3	93.70	28.47
CWFL-3 Prox	93.98	46.35
CWFL-4	68.86	-
CWFL-4 Prox	71.13	-

TABLE I: Average accuracy for MNIST and CIFAR dataset

accuracy are much more pronounced as compared to the IID case, which primarily happens due to noisy communication links. For the given range of SNR, COTAF fails to converge while CWFL demonstrated improved robustness and early convergence due to the large weightage given to the high-SNR cluster. The average accuracy depicted in Table I demonstrates that CWFL achieves improved accuracy and robustness, in addition to using fewer time-slots for communication as compared to the decentralised scheme.

VI. CONCLUSION AND FUTURE WORK

In scenarios where a powerful central server is absent, we proposed CWFL which employs SNR-based Kmeans algorithm for data-agnostic clustering of the clients. We showed that CWFL is a convergent FL scheme ($\mathcal{O}(1/T)$) that requires fewer channel uses as compared to decentralized FL. Using the MNIST and CIFAR datasets, we demonstrated that CWFL outperforms COTAF with respect to accuracy and robustness. Since improvements are substantial while using a proximal constraint, we plan to analyse the behavior of CWFL with the proximal constraint in future.

REFERENCES

- [1] Brendan McMahan, Eider Moore, Daniel Ramage, Seth Hampson, and Blaise Aguera y Arcas, “Communication-efficient learning of deep networks from decentralized data,” in *Artificial intelligence and statistics*. PMLR, 2017, pp. 1273–1282.
- [2] Jakub Konečný, H Brendan McMahan, Felix X Yu, Peter Richtárik, Ananda Theertha Suresh, and Dave Bacon, “Federated learning: Strategies for improving communication efficiency,” *arXiv preprint arXiv:1610.05492*, 2016.
- [3] Mohammad Mohammadi Amiri, Deniz Gündüz, Sanjeev R Kulkarni, and H Vincent Poor, “Convergence of federated learning over a noisy downlink,” *IEEE Transactions on Wireless Communications*, 2021.
- [4] Hong Xing, Osvaldo Simeone, and Suzhi Bi, “Federated learning over wireless device-to-device networks: Algorithms and convergence analysis,” *arXiv preprint arXiv:2101.12704*, 2021.

- [5] Tomer Sery, Nir Shlezinger, Kobi Cohen, and Yonina C. Eldar, “Cotaf: Convergent over-the-air federated learning,” in *GLOBECOM 2020*, 2020, pp. 1–6.
- [6] Tian Li, Anit Kumar Sahu, Manzil Zaheer, Maziar Sanjabi, Ameet Talwalkar, and Virginia Smith, “Federated optimization in heterogeneous networks,” *arXiv preprint arXiv:1812.06127*, 2018.
- [7] Xinwei Zhang, Mingyi Hong, Sairaj Dhople, Wotao Yin, and Yang Liu, “Fedpd: A federated learning framework with adaptivity to non-iid data,” *IEEE TSP*, 2021.
- [8] Xiang Li, Kaixuan Huang, Wenhao Yang, Shusen Wang, and Zhihua Zhang, “On the convergence of fedavg on non-iid data,” in *ICLR*, 2019.
- [9] Anusha Lalitha, Osman Cihan Kilinc, Tara Javidi, and Farinaz Koushanfar, “Peer-to-peer federated learning on graphs,” *arXiv preprint arXiv:1901.11173*, 2019.
- [10] Abhijit Guha Roy, Shayan Siddiqui, Sebastian Pölsterl, Nassir Navab, and Christian Wachinger, “Braintorrent: A peer-to-peer environment for decentralized federated learning,” *ArXiv*, vol. abs/1905.06731, 2019.
- [11] Chaoyang He, Conghui Tan, Hanlin Tang, Shuang Qiu, and Ji Liu, “Central server free federated learning over single-sided trust social networks,” 2021.
- [12] Muhammad Shayan, Clement Fung, Chris J. M. Yoon, and Ivan Beschastnikh, “Biscotti: A ledger for private and secure peer-to-peer machine learning,” *ArXiv*, vol. abs/1811.09904, 2018.
- [13] Mohammad Mohammadi Amiri and Deniz Gündüz, “Federated learning over wireless fading channels,” *IEEE Transactions on Wireless Communications*, vol. 19, no. 5, pp. 3546–3557, 2020.
- [14] Frank Po-Chen Lin, Seyyedali Hosseinalipour, Sheikh Shams Azam, Christopher G Brinton, and Nicolo Michelusi, “Semi-decentralized federated learning with cooperative d2d local model aggregations,” *IEEE Journal on Selected Areas in Communications*, vol. 39, no. 12, pp. 3851–3869, 2021.
- [15] Stefano Marano, Vincenzo Matta, Lang Tong, and Peter Willett, “A likelihood-based multiple access for estimation in sensor networks,” *IEEE Transactions on Signal Processing*, vol. 55, no. 11, pp. 5155–5166, 2007.
- [16] Kobi Cohen and Amir Leshem, “Performance analysis of likelihood-based multiple access for detection over fading channels,” *IEEE Transactions on Information Theory*, vol. 59, no. 4, pp. 2471–2481, 2012.
- [17] Mohammad Mohammadi Amiri and Deniz Gündüz, “Machine learning at the wireless edge: Distributed stochastic gradient descent over-the-air,” *IEEE TSP*, vol. 68, pp. 2155–2169, 2020.
- [18] Kai Yang, Tao Jiang, Yuanming Shi, and Zhi Ding, “Federated learning via over-the-air computation,” *IEEE Transactions on Wireless Communications*, vol. 19, no. 3, pp. 2022–2035, 2020.
- [19] Yandong Shi, Yong Zhou, and Yuanming Shi, “Over-the-air decentralized federated learning,” *arXiv preprint arXiv:2106.08011*, 2021.
- [20] Anusha Lalitha, Shubhanshu Shekhar, Tara Javidi, and Farinaz Koushanfar, “Fully decentralized federated learning,” in *Bayesian Deep Learning (NeurIPS)*, 2018.
- [21] Xiangru Lian, Ce Zhang, Huan Zhang, Cho-Jui Hsieh, Wei Zhang, and Ji Liu, “Can decentralized algorithms outperform centralized algorithms? a case study for decentralized parallel stochastic gradient descent,” *NeurIPS*, vol. 30, 2017.
- [22] David Tse and Pramod Viswanath, *Fundamentals of wireless communication*, Cambridge university press, 2005.

APPENDIX

We demonstrate the convergence of the CWFL framework using the following assumptions:

- 1) f_1, \dots, f_K are L -Lipschitz-smooth functions, i.e., $\forall \boldsymbol{\theta}, \boldsymbol{\vartheta} \in \mathbb{R}^d$,

$$f_k(\boldsymbol{\theta}) \leq f_k(\boldsymbol{\vartheta}) + (\boldsymbol{\theta} - \boldsymbol{\vartheta})^T \nabla f_k(\boldsymbol{\vartheta}) + \frac{L}{2} \|\boldsymbol{\theta} - \boldsymbol{\vartheta}\|^2.$$

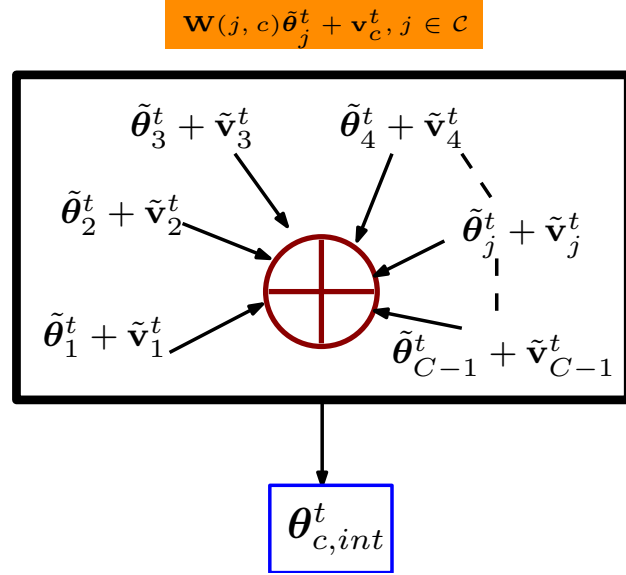


Fig. 3: The intermediate step $\bar{\theta}_c^{t+\frac{1}{2}}$

- 2) f_1, \dots, f_K are μ -strongly convex functions, i.e., $\forall \boldsymbol{\theta}, \boldsymbol{\vartheta} \in \mathbb{R}^d$,

$$f_k(\boldsymbol{\theta}) \geq f_k(\boldsymbol{\vartheta}) + (\boldsymbol{\theta} - \boldsymbol{\vartheta})^T \nabla f_k(\boldsymbol{\vartheta}) + \frac{\mu}{2} \|\boldsymbol{\theta} - \boldsymbol{\vartheta}\|^2.$$
- 3) Bounded variance: For uniformly sampled clients $k \sim \mathcal{U}([K])$, there exists a constant α_k such that the variance of stochastic gradients at each client is bounded, i.e.,

$$\mathbb{E} \|\nabla f_k(\boldsymbol{\theta}) - \nabla f_k(\boldsymbol{\theta}; \mathcal{D}_k)\|^2 \leq \alpha_k^2$$
 for $k \in [K]$. Here, $\nabla f_k(\boldsymbol{\theta}; \mathcal{D}_k)$ is the gradient w.r.t. entire data at the k -th client.
- 4) The expected squared norm of stochastic gradients is uniformly bounded, i.e.,

$$\mathbb{E} \|\nabla f_k(\boldsymbol{\theta})\|^2 \leq G^2$$
 for $k \in [K]$

Lemma 1. For any three vectors $\mathbf{a}, \mathbf{b}, \mathbf{c}$,

$$\|\mathbf{a} - \mathbf{b}\|^2 \leq 2\|\mathbf{a} - \mathbf{c}\|^2 + 2\|\mathbf{c} - \mathbf{b}\|^2 \quad (11)$$

Proof: We know that $(\mathbf{a} + \mathbf{b} - \mathbf{c})^T(\mathbf{a} + \mathbf{b} - \mathbf{c}) \geq 0$ which implies that $-2\mathbf{a}^T\mathbf{b} \leq \mathbf{a}^T\mathbf{a} + \mathbf{b}^T\mathbf{b} + 4\mathbf{c}^T\mathbf{c} - 4\mathbf{a}^T\mathbf{c} - 4\mathbf{b}^T\mathbf{c}$. We obtain the result given above by adding $\mathbf{a}^T\mathbf{a} + \mathbf{b}^T\mathbf{b}$ to both sides. \blacksquare

Lemma 2. The effective distribution across time slots $c \in \mathcal{C}$ in \mathbf{v}_c^t can be given using $\mathbf{v} \sim \mathcal{N}(0, \sum_{j=1}^C \mathbf{W}(c, j) \sigma_c^2)$.

Proof. Communication in the consensus phase happens across $(C - 1)$ time slots, where the

signal from the j -th cluster-head is given by $\tilde{\boldsymbol{\theta}}_j^t + \tilde{\mathbf{v}}_j^t$, where $\tilde{\mathbf{v}}_j^t \sim \mathcal{N}(0, \sigma_c^2)$. We consider an equivalent communication model, where we define $\boldsymbol{\theta}_{c,int}^t$ as given in fig. 3.

$$\begin{aligned}\boldsymbol{\theta}_{c,int}^t &= \sum_{j=1}^C \mathbf{W}(c, j) \left[\tilde{\boldsymbol{\theta}}_j^t + \tilde{\mathbf{v}}_j^t \right] \\ &= \sum_{j=1}^C \mathbf{W}(c, j) \tilde{\boldsymbol{\theta}}_j^t + \mathbf{v}_c^t\end{aligned}\quad (12)$$

where the effective noise vector $\mathbf{v}_c^t = \sum_{j=1}^C \mathbf{W}(c, j) \tilde{\mathbf{v}}_j^t$ such that $\mathbf{v}_c^t \sim \mathcal{N}(0, \kappa_c^2)$, where $\kappa_c^2 = \sum_{j=1}^C \mathbf{W}(c, j) \sigma_c^2$. \square

Theorem 1. *Under assumptions 1-4 given above, given constants L, μ, α_k, G, p_k , choosing $\gamma = \max(E, \frac{12L}{\mu})$ and choosing the learning rate $\eta^t = \frac{2}{\mu(\gamma+t)}$, each cluster in CWFL satisfies*

$$\mathbb{E} \|\tilde{\boldsymbol{\theta}}_c^T - \boldsymbol{\theta}^*\|^2 \leq \frac{2 \max(4(Q_1), \mu^2 \gamma \|\tilde{\boldsymbol{\theta}}_c^0 - \boldsymbol{\theta}^*\|^2)}{\mu^2 (T + \gamma - 1)} + Q_2, \quad (13)$$

where $Q_1 = 8E^2 G^2 \sum_{k \in \mathcal{K}_c^V} p_k + 6L\Gamma + \sum_{k \in \mathcal{K}_c^V} p_k^2 \alpha_k^2$, and

$$Q_2 = d(P^{-1} \sigma_c^2 + \kappa_c^2) + 3P^{-1} \sum_{j=1}^C (\mathbf{W}(c, j))^2 \left[\sum_{k_j \in \mathcal{K}_j^V} (p_{k_j})^2 + d\sigma_j^2 \right].$$

Proof. From (8), we have :

$$\tilde{\boldsymbol{\theta}}_c^t \triangleq \sum_{k \in \mathcal{K}_c^V} p_k \boldsymbol{\theta}_k^t + \tilde{\mathbf{w}}_c^t \mathbf{1}_{t \in \mathcal{H}}, \quad (14)$$

where $\mathbf{1}_{(\cdot)}$ is the indicator function and $p_k = \begin{cases} \sqrt{\frac{P_k}{P}}, & \text{if } k \in \mathcal{K}_c \\ 1, & \text{if } k \in \mathcal{V} \end{cases}$. We write $\hat{\mathbf{w}}_c^t = \tilde{\mathbf{w}}_c^t \mathbf{1}_{t \in \mathcal{H}}$. Next we define

$$\mathbf{g}^t \triangleq \sum_{k \in \mathcal{K}_c^V} p_k \nabla f(\boldsymbol{\theta}_k^t), \quad \bar{\mathbf{g}}^t \triangleq \sum_{k \in \mathcal{K}_c^V} p_k \nabla F(\boldsymbol{\theta}_k^t). \quad (15)$$

It also follows $\mathbb{E}[\mathbf{g}^t] = \bar{\mathbf{g}}^t$. Consequently,

$$\tilde{\boldsymbol{\theta}}_c^{t+1} = \bar{\boldsymbol{\theta}}_c^t - \eta^t \mathbf{g}^t + \hat{\mathbf{w}}_c^t. \quad (16)$$

The above equation differentiates our proof from previous works such as [5], [8]. Since previous works are server-based, $\tilde{\boldsymbol{\theta}}_c^{t+1}$ would depend upon the local copy ($\tilde{\boldsymbol{\theta}}_c^t$ of the previous global update $\boldsymbol{\theta}^t$). However, since CWFL assigns a consensus update as the global update, $\tilde{\boldsymbol{\theta}}_c^t$ is replaced by $\bar{\boldsymbol{\theta}}_c^t$, in the virtual sequence. Note that $\bar{\boldsymbol{\theta}}_c^t = \boldsymbol{\theta}_k^t \forall k \in \mathcal{K}_c^V$, when $t \in \mathcal{H}$. The noise vector \mathbf{w} satisfies,

$$\mathbb{E} [\|\hat{\mathbf{w}}_c^t\|^2] = \mathbb{E} [\|\tilde{\mathbf{w}}_c^t \mathbf{1}_{t \in \mathcal{H}}\|^2] = \frac{d\sigma_c^2}{P} \mathbf{1}_{t \in \mathcal{H}}. \quad (17)$$

Note that $\bar{\boldsymbol{\theta}}_c^t = \tilde{\boldsymbol{\theta}}_c^t + \sum_{j=1}^C \mathbf{W}(c, j) \tilde{\boldsymbol{\theta}}_j^t + \mathbf{v}_c^t$. Expanding term T2,

$$\begin{aligned}
\|\tilde{\boldsymbol{\theta}}_c^{t+1} - \boldsymbol{\theta}^*\|^2 &= \|\bar{\boldsymbol{\theta}}_c^t - \eta^t \mathbf{g}^t - \boldsymbol{\theta}^* + \mathbf{w}_c^t\|^2 \\
&= \|\tilde{\boldsymbol{\theta}}_c^t + \sum_{j=1}^C \mathbf{W}(c, j) \tilde{\boldsymbol{\theta}}_j^t + \mathbf{v}_c^t - \eta^t \mathbf{g}^t - \boldsymbol{\theta}^* + \eta^t \bar{\mathbf{g}}^t - \eta^t \bar{\mathbf{g}}^t + \mathbf{w}_c^t\|^2 \\
&= \underbrace{\|\tilde{\boldsymbol{\theta}}_c^t + \sum_{j=1}^C \mathbf{W}(c, j) \tilde{\boldsymbol{\theta}}_j^t - \eta^t \bar{\mathbf{g}}^t - \boldsymbol{\theta}^*\|^2}_{\text{T3}} + \underbrace{(\eta^t)^2 \|\bar{\mathbf{g}}^t - \mathbf{g}^t + \frac{\mathbf{w}_c^t}{\eta^t} + \frac{\mathbf{v}_c^t}{\eta^t}\|^2}_{\text{T4}} \\
&\quad + \underbrace{2\eta^t \langle \tilde{\boldsymbol{\theta}}_c^t + \sum_{j=1}^C \mathbf{W}(c, j) \tilde{\boldsymbol{\theta}}_j^t - \boldsymbol{\theta}^* - \eta^t \bar{\mathbf{g}}^t, \bar{\mathbf{g}}^t - \mathbf{g}^t + \frac{\mathbf{w}_c^t}{\eta^t} + \frac{\mathbf{v}_c^t}{\eta^t} \rangle}_{\text{Expectation of this term goes to zero}}. \quad (18)
\end{aligned}$$

We bound term T3 as,

$$\begin{aligned}
\left\| \tilde{\boldsymbol{\theta}}_c^t + \sum_{j=1}^C \mathbf{W}(c, j) \tilde{\boldsymbol{\theta}}_j^t - \eta^t \bar{\mathbf{g}}^t - \boldsymbol{\theta}^* \right\|^2 &= \left\| \tilde{\boldsymbol{\theta}}_c^t - \boldsymbol{\theta}^* \right\|^2 + \underbrace{\left\| \sum_{j=1}^C \mathbf{W}(c, j) \tilde{\boldsymbol{\theta}}_j^t - \eta^t \bar{\mathbf{g}}^t \right\|^2}_{\text{T5}} \\
&\quad + \underbrace{2 \langle \tilde{\boldsymbol{\theta}}_c^t - \boldsymbol{\theta}^*, \sum_{j=1}^C \mathbf{W}(c, j) \tilde{\boldsymbol{\theta}}_j^t - \eta^t \bar{\mathbf{g}}^t \rangle}_{\text{T6}}. \quad (19)
\end{aligned}$$

Using Lemma 1, term T5 can be written as,

$$\left\| \sum_{j=1}^C \mathbf{W}(c, j) \tilde{\boldsymbol{\theta}}_j^t - \eta^t \bar{\mathbf{g}}^t \right\|^2 \leq 2 \left\| \sum_{j=1}^C \mathbf{W}(c, j) \tilde{\boldsymbol{\theta}}_j^t \right\|^2 + 2 \|\eta^t \bar{\mathbf{g}}^t\|^2. \quad (20)$$

Further, expanding T6 we obtain

$$\begin{aligned}
2 \langle \tilde{\boldsymbol{\theta}}_c^t - \boldsymbol{\theta}^*, \sum_{j=1}^C \mathbf{W}(c, j) \tilde{\boldsymbol{\theta}}_j^t - \eta^t \bar{\mathbf{g}}^t \rangle &\leq 2 \langle \tilde{\boldsymbol{\theta}}_c^t - \boldsymbol{\theta}^*, \sum_{j=1}^C \mathbf{W}(c, j) \tilde{\boldsymbol{\theta}}_j^t \rangle - 2 \langle \tilde{\boldsymbol{\theta}}_c^t - \boldsymbol{\theta}^*, \eta^t \bar{\mathbf{g}}^t \rangle \\
&\leq -2 \langle \boldsymbol{\theta}^* - \tilde{\boldsymbol{\theta}}_c^t, \sum_{j=1}^C \mathbf{W}(c, j) \tilde{\boldsymbol{\theta}}_j^t \rangle - 2 \langle \tilde{\boldsymbol{\theta}}_c^t - \boldsymbol{\theta}^*, \eta^t \bar{\mathbf{g}}^t \rangle \\
&\leq \left\| \tilde{\boldsymbol{\theta}}_c^t - \boldsymbol{\theta}^* \right\|^2 + \left\| \sum_{j=1}^C \mathbf{W}(c, j) \tilde{\boldsymbol{\theta}}_j^t \right\|^2 - 2 \langle \tilde{\boldsymbol{\theta}}_c^t - \boldsymbol{\theta}^*, \eta^t \bar{\mathbf{g}}^t \rangle. \quad (21)
\end{aligned}$$

Now (19) can be written as,

$$\begin{aligned}
\left\| \tilde{\boldsymbol{\theta}}_c^t + \sum_{j=1}^C \mathbf{W}(c, j) \tilde{\boldsymbol{\theta}}_j^t - \eta^t \bar{\mathbf{g}}^t - \boldsymbol{\theta}^* \right\|^2 &\leq 2 \left\| \tilde{\boldsymbol{\theta}}_c^t - \boldsymbol{\theta}^* \right\|^2 + 3 \left\| \sum_{j=1}^C \mathbf{W}(c, j) \tilde{\boldsymbol{\theta}}_j^t \right\|^2 \\
&\quad + \underbrace{2 \|\eta^t \bar{\mathbf{g}}^t\|^2}_{\text{T7}} - \underbrace{2 \langle \tilde{\boldsymbol{\theta}}_c^t - \boldsymbol{\theta}^*, \eta^t \bar{\mathbf{g}}^t \rangle}_{\text{T8}}. \quad (22)
\end{aligned}$$

For obtaining an upper bound for terms T7 and T8, we follow the steps derived in the proof of [8] and [5]. We assume $\eta^t \leq \frac{1}{6L}$, and hence, $6L(\eta^t)^2 \leq \eta_t$. It implies that $6L(\eta^t)^2 - 2\eta^t \leq \eta^t - 2\eta^t \leq -\eta^t$. It also implies $\eta^t L - 1 \leq \frac{-5}{6}$ and $2\eta^t - 6L(\eta^t)^2 \leq 2\eta^t$. Consequently, the final bound in (22) becomes,

$$\begin{aligned} \left\| \tilde{\boldsymbol{\theta}}_c^t + \sum_{j=1}^C \mathbf{W}(c, j) \tilde{\boldsymbol{\theta}}_j^t - \eta^t \bar{\mathbf{g}}^t - \boldsymbol{\theta}^* \right\|^2 &\leq (2 - \mu\eta^t) \|\tilde{\boldsymbol{\theta}}_c^t - \boldsymbol{\theta}^*\|^2 + 3 \left\| \sum_{j=1}^C \mathbf{W}(c, j) \tilde{\boldsymbol{\theta}}_j^t \right\|^2 + \\ &2 \sum_{k \in \mathcal{K}_c^V} p_k \|(\tilde{\boldsymbol{\theta}}_c^t - \boldsymbol{\theta}_k^t)\|^2 + 6L(\eta^t)^2 \Gamma - \frac{5\eta^t}{3} (F(\tilde{\boldsymbol{\theta}}_c^t) - F^*). \end{aligned} \quad (23)$$

We substitute (23) back to (18) and take expectation over the resulting inequality. Note that the expectation over the inner product term in (18) results zero.

$$\begin{aligned} \mathbb{E} \left[\|\tilde{\boldsymbol{\theta}}_c^{t+1} - \boldsymbol{\theta}^*\|^2 \right] &\leq (2 - \mu\eta^t) \mathbb{E} \left[\|\tilde{\boldsymbol{\theta}}_c^t - \boldsymbol{\theta}^*\|^2 \right] + 3 \mathbb{E} \left\| \sum_{j=1}^C \mathbf{W}(c, j) \tilde{\boldsymbol{\theta}}_j^t \right\|^2 + 2 \sum_{k \in \mathcal{K}_c^V} p_k \mathbb{E} \left[\|(\tilde{\boldsymbol{\theta}}_c^t - \boldsymbol{\theta}_k^t)\|^2 \right] \\ &+ 6L(\eta^t)^2 \Gamma - \frac{5\eta^t}{3} \mathbb{E} \left[(F(\tilde{\boldsymbol{\theta}}_c^t) - F^*) \right] + (\eta^t)^2 \mathbb{E} \left[\left\| \left(\mathbf{g}^t - \bar{\mathbf{g}}^t + \frac{\mathbf{w}_c^t}{\eta^t} + \frac{\mathbf{v}_c^t}{\eta^t} \right) \right\|^2 \right]. \end{aligned} \quad (24)$$

The second term in the RHS above can be written as,

$$\begin{aligned} \mathbb{E} \left\| \sum_{j=1}^C \mathbf{W}(c, j) \tilde{\boldsymbol{\theta}}_j^t \right\|^2 &\leq \sum_{j=1}^C (\mathbf{W}(c, j))^2 \mathbb{E} \left\| \tilde{\boldsymbol{\theta}}_j^t \right\|^2 \leq \sum_{j=1}^C (\mathbf{W}(c, j))^2 \left[\sum_{k_j \in \mathcal{K}_j^V} \frac{(p_{k_j})^2 P_{k_j}}{P_{k_j}^t} + \frac{d\sigma_j^2}{P} \right] \\ &\leq P^{-1} \sum_{j=1}^C (\mathbf{W}(c, j))^2 \left[\sum_{k_j \in \mathcal{K}_j^V} (p_{k_j})^2 + d\sigma_j^2 \right]. \end{aligned} \quad (25)$$

Since the noise vectors $\mathbf{w}_c^t, \mathbf{v}_c^t$ are zero-mean and statistically independent of \mathbf{g}^t and $\bar{\mathbf{g}}^t$, we can simplify T4 in (18) as follows:

$$\begin{aligned} \mathbb{E} \left[\left\| \bar{\mathbf{g}}^t - \mathbf{g}^t + \frac{\mathbf{w}_c^t}{\eta^t} + \frac{\mathbf{v}_c^t}{\eta^t} \right\|^2 \right] &= \mathbb{E} \left[\left\| \bar{\mathbf{g}}^t - \mathbf{g}^t \right\|^2 \right] + \mathbb{E} \left[\left\| \frac{\mathbf{w}_c^t}{\eta^t} \right\|^2 \right] + \mathbb{E} \left[\left\| \frac{\mathbf{v}_c^t}{\eta^t} \right\|^2 \right], \\ &\leq \sum_{k \in \mathcal{K}_c^V} p_k^2 \alpha_k^2 + \mathbb{E} \left[\left\| \frac{\mathbf{w}_c^t}{\eta^t} \right\|^2 \right] + \mathbb{E} \left[\left\| \frac{\mathbf{v}_c^t}{\eta^t} \right\|^2 \right], \\ &\leq \sum_{k \in \mathcal{K}_c^V} p_k^2 \alpha_k^2 + \frac{d\sigma_c^2}{P(\eta^t)^2} \mathbb{1}_{t \in \mathcal{H}} + \frac{d\kappa_c^2}{(\eta^t)^2}, \\ &\leq \sum_{k \in \mathcal{K}_c^V} p_k^2 \alpha_k^2 + \frac{d\sigma_c^2}{P(\eta^t)^2} \mathbb{1}_{t \in \mathcal{H}} + \frac{d\kappa_c^2}{(\eta^t)^2}. \end{aligned} \quad (26)$$

In the above, we use assumption 3 and the definitions of \mathbf{g}^t and $\bar{\mathbf{g}}^t$. Following the proof in [5] and references therein, when $\eta^t \leq 2\eta^{t+E}$ for all $t \geq 0$ and when assumption 3 holds,

$$\sum_{k \in \mathcal{K}_c^{\mathcal{V}}} p_k \mathbb{E} \left[\|\tilde{\boldsymbol{\theta}}_c^t - \boldsymbol{\theta}_k^t\|^2 \right] \leq 4(\eta^t)^2 G^2 E^2 \sum_{k \in \mathcal{K}_c^{\mathcal{V}}} p_k. \quad (27)$$

Putting together equations (24), (25), (26) and (27),

$$\begin{aligned} \mathbb{E} \left[\|\tilde{\boldsymbol{\theta}}_c^{t+1} - \boldsymbol{\theta}^*\|^2 \right] &\leq (2 - \mu\eta^t) \mathbb{E} \left[\|\tilde{\boldsymbol{\theta}}_c^t - \boldsymbol{\theta}^*\|^2 \right] + 3P^{-1} \sum_{j=1}^C (\mathbf{W}(c, j))^2 \left[\sum_{k_j \in \mathcal{K}_j^{\mathcal{V}}} (p_{k_j})^2 + d\sigma_j^2 \right] \\ &+ 8(\eta^t)^2 E^2 G^2 \sum_{k \in \mathcal{K}_c^{\mathcal{V}}} p_k + 6L(\eta^t)^2 \Gamma - \frac{5\eta^t}{3} \mathbb{E} \left[(F(\tilde{\boldsymbol{\theta}}_c^t) - F^*) \right] \\ &+ (\eta^t)^2 \left[\sum_{k \in \mathcal{K}_c^{\mathcal{V}}} p_k^2 \alpha_k^2 + \underbrace{\frac{d\sigma_c^2}{P^2(\eta^t)^2} \mathbb{1}_{t \in \mathcal{H}}}_{\mathbf{D}} + \frac{d\kappa_c^2}{(\eta^t)^2} \right]. \end{aligned} \quad (28)$$

We define $\delta^t \triangleq \mathbb{E} \|\tilde{\boldsymbol{\theta}}_c^t - \boldsymbol{\theta}^*\|^2$, which gives us a recursive relation similar to [5]. Further since $-\eta^t \mathbb{E} \left[F(\tilde{\boldsymbol{\theta}}_c^t) - F^* \right] \leq 0$ and as $\mathbf{D} \mathbb{1}_{t \in \mathcal{H}} \leq \mathbf{D}$ for $\mathbf{D} \geq 0$. We set the step size $\eta^t = \frac{\rho}{(t+\gamma)}$ for some $\rho > \frac{1}{\mu}$ and $\gamma \geq \max(6L\rho, E)$, for which $\eta^t \leq \frac{1}{6L}$ and $\eta^t \leq 2\eta^{t+E}$

$$\delta^{t+1} \leq (2 - \mu\eta^t)\delta^t + (\eta^t)^2 Q_1 + Q_2 \leq (1 - \mu\eta^t)\delta^t + (\eta^t)^2 Q_1 + \delta^t + Q_2 \quad (29)$$

where,

$$\begin{aligned} Q_1 &= 8E^2 G^2 \sum_{k \in \mathcal{K}_c^{\mathcal{V}}} p_k + 6L\Gamma + \sum_{k \in \mathcal{K}_c^{\mathcal{V}}} p_k^2 \alpha_k^2, \\ Q_2 &= 3P^{-1} \sum_{j=1}^C (\mathbf{W}(c, j))^2 \left[\sum_{k_j \in \mathcal{K}_j^{\mathcal{V}}} (p_{k_j})^2 + d\sigma_j^2 \right] + \frac{d\sigma_c^2}{P} + d\kappa_c^2. \end{aligned}$$

Note that a similar expression for recursion is obtained in [5]. However, in contrast, the expression for Q_1 is different, while we have an additional term Q_2 as well.

In [5], it is already shown using induction that if $\nu \geq \frac{\rho^2 Q}{\rho\mu-1}$, $\nu \geq \gamma\delta^0$ and $\delta^t \leq \frac{\nu}{t+\gamma}$, then $\delta^{t+1} \leq \frac{\nu}{t+1+\gamma}$ holds. Further note that Q_2 and δ^t are always positive. It is also true that, $\delta^{t+1} \leq$

$\frac{\nu}{t+1+\gamma} + \frac{\nu}{t+\gamma} + Q_2$. This holds for $\nu = \max\left(\frac{\rho^2 Q_1}{\rho\mu-1}, \gamma\delta^0\right)$, $\gamma \geq \max(E, 6\rho L)$ and $\rho > 0$. Further, by setting $\rho = \frac{2}{\mu}$ we have $\gamma = \max\left(E, \frac{12L}{\mu}\right)$, $\nu = \max\left(\frac{4Q_1}{\mu^2}, \gamma\delta^0\right)$ and hence,

$$\begin{aligned}\mathbb{E} \left[\|\tilde{\boldsymbol{\theta}}_c^{t+1} - \boldsymbol{\theta}^*\|^2 \right] &\leq \frac{\max(4Q_1, \mu^2\gamma\delta^0)}{\mu^2(t+1+\gamma)} + \frac{\max(4Q_1, \mu^2\gamma\delta^0)}{\mu^2(t+\gamma)} + Q_2 \\ &= \max(4Q_1, \mu^2\gamma\delta^0) \frac{2t+2\gamma+1}{\mu^2(t+1+\gamma)(t+\gamma)} + Q_2 \\ &\leq \frac{2\max(4Q_1, \mu^2\gamma\delta^0)}{t+\gamma} + Q_2.\end{aligned}\tag{30}$$

This completes the proof for theorem 1. Note that when ξ_c is large, cluster $c \in \mathcal{C}$ is an SNR dominant cluster and we can say $\sigma_c^2 \rightarrow 0$. From lemma 2, we know $\kappa_c^2 \rightarrow 0$ in such scenarios. Further, the product, $\mathbf{W}(c, j)^2 \sigma_j^2 \approx 0$ at high SNR for $c \neq j$. Since $\mathbf{W}(c, j) = \frac{\xi_j}{\sum_{j=1}^C \xi_j}$, and $\xi_c \gg \xi_j$ for all $j \neq c$, $\mathbf{W}(c, j) \approx 0$ for all $j \neq c$. This further implies that $Q_2 \approx 0$. Hence, for the high-SNR cluster with $\xi_c \gg \xi_j$, convergence occurs as $\mathcal{O}(1/T)$. \square